



Geneeskundige Stichting Koningin Elisabeth  
Fondation Médicale Reine Elisabeth  
Königin-Elisabeth-Stiftung für Medizin  
Queen Elisabeth Medical Foundation

Final report  
of the research group of

---

Prof. Vanhollebeke Benoit, PhD

Université Libre de Bruxelles (ULB)

## Principal investigator

---

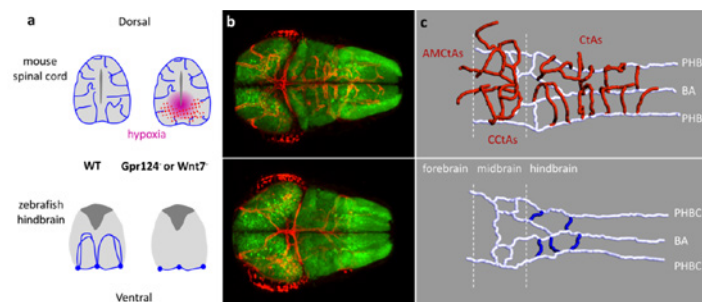
Prof. Vanhollebeke Benoit, PhD  
Head of the Laboratory of Neurovascular Signaling  
Department of Molecular Biology  
Neuroscience Institute Faculty of Sciences  
University of Brussels (ULB)  
Tel.: +32 2 650 97 61  
Fax: +32 2 650 97 50  
E-mail: [Benoit.Vanhollebeke@ulb.ac.be](mailto:Benoit.Vanhollebeke@ulb.ac.be)  
[nvasc.ulb.be/vanhollebekelab/](http://nvasc.ulb.be/vanhollebekelab/)

# Organ-wide analysis of brain neurovascular communication in real-time and at single-cell resolution

## 1. State of the Art

Blood vessels are more than passive conduits for blood flow and that tissue-specific vascular beds not only match the metabolic demands of the perfused organs, but also act as important signaling centers releasing angiocrine factors that contribute to organ development, maintenance and repair. Accordingly, proper brain function relies on elaborate communications between the neural and vascular system and this organ serves as a paradigm for extensive crosstalk between the vascular system and its local microenvironment. Central nervous system (CNS) neurovascular development has been best studied in the developing mouse CNS and a number of genetic regulators of neurovascular development have been uncovered, with a subset of them further organized into networks. Despite this progress, an integrated picture of how, when and to what extent neural and vascular development are coordinated is lacking. Building this model will critically rely on the combined capacity to (i) scrutinize the cellular modalities of the intrinsically highly dynamic processes of vascular and neural development in real-time and to (ii) identify experimental settings where the signaling and circulatory functions of the intracerebral blood vessels can be, at least partially, uncoupled. Every aspect of neurovascular development and function, from blood vessels morphogenesis and BBB formation to neural cell metabolism, is indeed exquisitely sensitive to reduced tissue oxygen tension. The hypoxia response that invariably accompanies defective vascular development is a confounding factor severely blunting the scope of approachable investigations in the field.

Our previous work identified and validated the optically-clear zebrafish embryonic brain as uniquely endowed with these distinctive attributes, through the startling observation that zebrafish brains remain normoxic throughout organogenesis even in the total absence of intracerebral blood vessels and that, after prolonged periods of impaired vascular development, blood vessels invade and branch within the neural system in stereotypical patterns, implying long-prevailing physiological conditions.



**A normoxic and transparent setting to explore CNS neurovascular interactions.** (a) Cross-section through the mouse and zebrafish central nervous system with or without impaired vascular development. (b) z-projection of a dorsal confocal scan through the zebrafish brain, with post-mitotic neurons labeled in green and endothelial cells in red. (c) Wire-diagram representation of WT and mutant zebrafish brain vasculature in dorso-lateral views. Red vessels represent the intra-cerebral BBB network.

Through the combined increase in spatio-temporal resolution, best suited to comprehend the intrinsically dynamic processes of neurovascular development and function, and the absence of confounding hypoxic signaling cascades, some fundamental questions seem now within reach: Through which cellular and molecular mechanisms is CNS vascular invasion and maturation controlled by neural signals? Reciprocally, how does the developing vascular system impact on brain patterning and function?

The physical and genetic constraints imposed to the study of the dynamic cellular mechanisms governing sprouting angiogenesis have restricted their investigation to a limited number of *in vivo* settings, most notably the postnatal mouse retina and the zebrafish ISVs. In recent years, a coherent model integrating controlled behaviors of VEGF-selected tip cells and notch-induced stalk cells within nascent sprouts has been derived from those prototypical settings. Hierarchical organization of differentially-fated endothelial cells (ECs) during sprouting angiogenesis and organ-specific adaptations are viewed as consecutive, and hence distinct, aspects of vascular development. However, through live imaging of mosaic animals, an integrated control was recently shown to operate under the control of CNS-derived signals. Neural progenitor-derived Wnt7 ligands, well-known inducers of brain EC maturation, govern CNS EC invasion through selective modulation of tip cell function within the parental perineural vessels.

## 2. Objectives

---

A major aim of our project is to address how the neural and vascular systems communicate to assemble functional neurovascular units. In particular, we study how perineural endothelial cells (ECs) selectively respond to neural-derived Wnt7 ligands during the process of brain angiogenesis.

From the initial discovery of Frizzled as Wnt receptors two decades ago to the recent crystallographic insights into their interaction mechanism, it has remained unknown how cells discriminate between multiple Wnt ligands within complex biological systems. The Wnt/Frizzled interaction chemistry is indeed incompatible with mono-specific recognition and, accordingly, when tested in pair-wise combinations, multiple Wnt ligands compete for binding to various Frizzled receptors. We are exploring a novel molecular mechanism that enables cells to bind and respond to Wnt7 ligands with strict specificity.

Our previous findings indeed identified Adgra2/Gpr124, an orphan member of the adhesion class of G protein-coupled receptors as an essential co-factor of Wnt7 signaling in CNS ECs. Adhesion G protein-coupled receptors (aGPCRs) constitute the second largest group of GPCRs in humans. Most aGPCRs are orphan receptors with no identified ligands that function through remarkably diverse mechanisms. They differ from other GPCRs by long N-terminal extensions preceding a membrane-proximal GPCR autoproteolysis-inducing (GAIN) domain containing the highly conserved GPCR proteolytic site (GPS). These N-terminal sequences typically comprise multiple protein-protein interaction domains involved in cell-cell and cell-matrix contacts. This structural hallmark significantly broadens the signaling potential and complexity of this class of GPCRs that, context-dependently, behave as adhesion molecules or signal transducing GPCRs. Gpr124, a member of this branch of GPCRs has gained considerable interest since the discovery of its essential role in brain vascular development (Kuhnert et al., 2010). Upon genetic inactivation, vascularization and blood-brain barrier maturation are impaired in all or parts of the zebrafish and mouse central nervous system, respectively (Anderson et al., 2011; Cullen et al., 2011; Kuhnert et al., 2010; Vanhollebeke et al., 2015). This receptor promotes angiogenic sprouting through endothelial cell (EC)-autonomous Wnt/ $\beta$ -catenin signaling stimulation upon contact with neural progenitor-derived Wnt7 ligands (Posokhova et al., 2015; Vanhollebeke et al., 2015; Zhou and Nathans, 2014).

Genetic studies in zebrafish have shown that in order to recognize these ligands, and hence to be competent for brain invasion, ECs must additionally express Reck, a GPI-anchored glycoprotein (Ulrich et al., 2016; Vanhollebeke et al., 2015). Consistently, EC-specific invalidation of RECK in the mouse leads to CNS-specific vascular defects, thereby demonstrating the evolutionary conserved role of RECK in cerebrovascular development (de Almeida et al., 2015). Gpr124 and Reck have been proposed to interact at the plasma membrane to assemble a potent and Wnt7-specific Wnt/ $\beta$ -catenin co-activator complex (Vanhollebeke et al., 2015). The complex also operates in neural crest-derived cells to promote

dorsal root ganglia (DRG) neurogenesis in zebrafish embryos (Vanhollebeke et al., 2015). Defective DRG neurogenesis is accompanied by metamorphic pigmentation alterations in the adult Gpr124 mutant skin (Vanhollebeke et al., 2015).

While the genetic interaction between *gpr124* (also known as *adgra2*) and *reck* is well supported by studies in the zebrafish model as well as cell culture experiments, their activation and signaling mechanisms are poorly characterized, in part as a result of a lack of *in vivo* models where structure-function relationships can be probed.

### 3. Results

---

#### 3.1. Identification of an *in vivo* model of *gpr124/adgra2*-dependent neurovascular dysfunction (Bostaille et al. *Development*)

---

Malmquist *et al.* (2013) phenotypically characterized the *ouchless* mutant that was recovered from an F3 forward genetic screen for defective dorsal root ganglion (DRG) neurogenesis in zebrafish. While the initial dorsoventral migration of neural crest-derived cell clusters towards presumptive DRG locales appears unaffected in *ouchless* mutants, the neurogenic program leading to the generation of *neurog1:EGFP+* cells within the ganglion is defective, resulting in a severe reduction of DRG numbers in 72 hours post fertilization (hpf) *ouchless* mutants. *ouchless* mutants are viable but exhibit reduced growth rates and interrupted melanophore stripes in the adult skin. The *ouchless* mutation was mapped by bulk segregation analysis to a 342 kb genomic region of chromosome 8, harboring the *sorbs3* gene. No causative mutation could be identified within the coding sequence of *sorbs3*, but a mutation was suspected to reside within cis-regulatory elements, accounting for the reduced *sorbs3* transcript levels observed in *ouchless* mutants. Antisense *sorbs3* morpholino knockdown experiments, as well as BAC and mRNA rescue experiments, further supported the model that *sorbs3* regulates DRG neurogenesis and that *sorbs3* dysfunction drives the *ouchless* phenotypes (Malmquist et al., 2013).

The *ouchless* phenotypes are remarkably analogous to the DRG defects reported in *gpr124* knock-out mutants (Vanhollebeke et al., 2015). Of note *gpr124* has been renamed to *adgra2*. Along with *Reck*, *Gpr124/Adgra2* has been shown to control DRG formation by activating Wnt signaling in neural crest-derived *sox10:mRFP+* ganglion cells (Vanhollebeke et al., 2015). Given the phenotypic similarities, we therefore set out to test whether *adgra2* and *ouchless* (presumably *sorbs3*) co-operate during the process of DRG neurogenesis and brain vascularization.

We first demonstrated that **adgra2/gpr124** and **ouchless** genetically interact by functional gene dosage experiments (**Figure 1**).

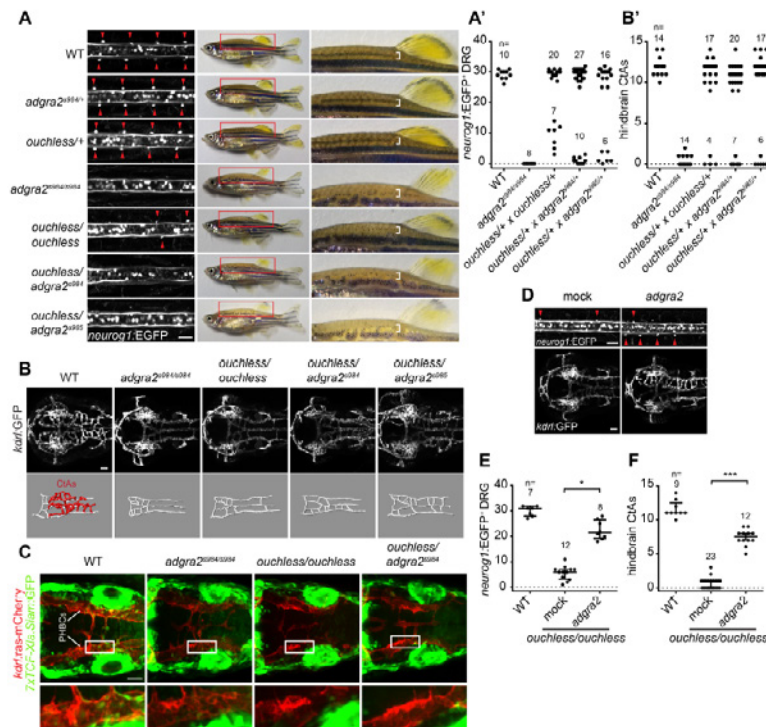


**Figure 1** *gpr124/adgra2* and *ouchless* mutations fail to complement. (A and A') Fish heterozygous for *ouchless* were crossed with the previously described *adgra2* heterozygotes, *adgra2*<sup>S984/+</sup> and *adgra2*<sup>S985/+</sup>, and the offspring were assessed at 72 hpf for defects in DRG neurogenesis. From these crosses, ~25% of the offspring (annotated as *ouchless/adgra2*<sup>S984</sup> and *ouchless/adgra2*<sup>S985</sup>) showed an almost complete lack of **neurog1:EGFP**<sup>+</sup> DRG. When raised to adulthood, these fish could be distinguished from their siblings by discontinuous dorsal melanophore stripes on their skin (brackets). (B and B') Cerebral vasculatures of 60 hpf embryos derived from *ouchless* heterozygotes incrosses and outcrosses to *adgra2* heterozygotes. 25% of the offspring of each of the crosses displays highly penetrant brain vascular defects, characterized by a complete absence of central arteries (CtAs), similar to *adgra2* mutants. (C) Defective endothelial Wnt/ $\beta$ -catenin signaling in the perineural primordial hindbrain channel (PHBC) ECs. (D-F) When *ouchless* mutants are injected at the one-cell stage with mRNA encoding wild-type (WT) *Adgra2*, significant restoration of **neurog1:EGFP**<sup>+</sup> DRG and cerebral blood vessels is observed.

The lack of complementation between *ouchless* and *adgra2*, together with the discovery of vascular phenotypes in *ouchless* mutants that mimic those of *adgra2* mutants, indicates that *ouchless* constitutes a new allele of *adgra2*. The re-evaluation of the genomic region known to harbour the *ouchless* mutation revealed that the *adgra2* gene resides within the critical interval, spanning the ca-48 and ca-37 genomic markers. In *ouchless* mutants, *adgra2* displays an essential splice site mutation inactivating *Adgra2* through the in-frame deletion of a single LRR in the ectodomain of this adhesion G-protein coupled receptor (Figure 2).

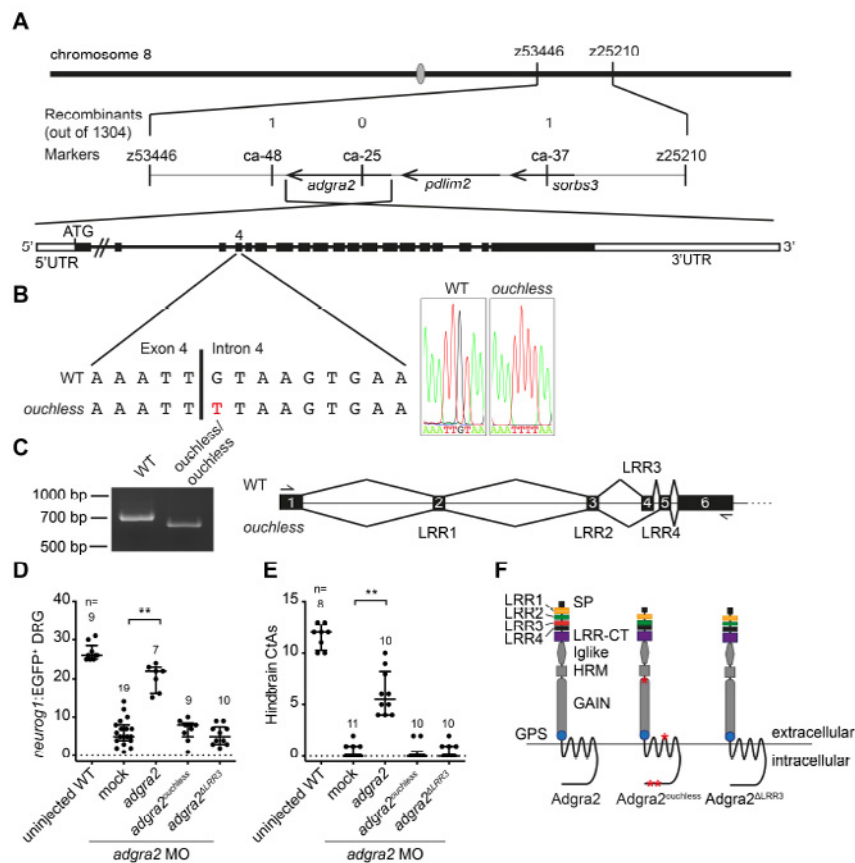


**Figure 2 *adgra2* is mutated in *ouchless* mutants.** (A) Representation of the *ouchless* locus genetic map on chromosome 8. The number of recombinants among 1304 meioses as determined by Malmquist et al. (2013) is indicated above the markers utilized for mapping. (B) Sanger sequencing of the exon 4-intron 4 boundary of *adgra2* in WT and *ouchless* mutant embryos. The G→T change in the *ouchless* 5' splice donor sequence appears in red. (C) RT-PCR splicing analysis of *adgra2* in 48 hpf WT and *ouchless* mutant embryos. The amplification primers hybridize to exon 1 and exon 6, as illustrated in the panel on the right. (D, E) The capacity of the full-length *adgra2* coding sequence from *ouchless* mutants to rescue DRG and CtA defects in *adgra2* morphants was evaluated by mRNA injection at the one-cell stage. While mRNA encoding the WT receptor (annotated as *adgra2*) partially suppressed both phenotypes, the *ouchless* variant (annotated as *adgra2<sup>ouchless</sup>*) did not affect either. (F) Comparison of a reference WT *adgra2* allele with the *adgra2* coding sequence recovered from *ouchless* mutant embryos. Four non-synonymous single nucleotide polymorphisms (SNPs; M429V, S895P, A1282V and A1302G) as well as an in-frame 72 bp deletion corresponding to exon 4 are found in *ouchless*. While all four *adgra2* SNPs identified in *ouchless* mutants had been previously identified in functionally validated *adgra2* alleles derived from mixed AB/TL genetic backgrounds, alternative splicing resulting in exon 4 skipping is absent from any known zebrafish, mouse or human *ADGRA2* isoform. When probed in zebrafish, alternative splicing of the exon 1-exon 6 sequences is undetectable by RT-PCR (C). Exon 4 corresponds precisely to the third leucine-rich repeat (LRR) unit of the LRR/CT domain of Adgra2, which comprises an array of four 24-residue-long LRR units followed by a LRR cysteine-rich C-terminal motif (LRR-CT).

Altogether, this work reveals that *ouchless* and *adgra2* mutants are allelic and that the *ouchless* phenotypes result from an essential splice site mutation inactivating Adgra2 through the in-frame deletion of a single LRR in the ectodomain of this adhesion G-protein coupled receptor (GPCR). The zebrafish *ouchless* mutant thereby constitutes the first *in vivo* model of *adgra2* N-terminal domain-specific variation.

### 3.2. Molecular insights into Adgra2/Gpr124 and Reck intracellular trafficking (Bostaille et al. Biology Open)

Taking advantage of the above-described mutation in *adgra2*, we undertook to better define the cellular and molecular modalities of the Gpr124/Reck synergistic interaction. In particular, the stoichiometry of the Gpr124/Reck complex and the molecular determinants of its trafficking, assembly and signal transduction still needed to be investigated. The N-terminal domains of Gpr124 are likely contributors to several, if not all, of these processes. Indeed, cell culture and *in vivo* experiments have revealed that Gpr124 function critically relies on its extracellular domain architecture. N-terminal truncations or substitution of the ectodomain of Gpr124 with the equivalent domain derived from the closely related

Gpr125, abrogate receptor signaling (Posokhova et al., 2015; Vanhollebeke et al., 2015). Moreover, the Gpr124 potential interaction interface with Reck, a cell surface exposed GPI-anchored glycoprotein, is restricted to the extracellular parts of the receptor.

As is typically found in aGPCRs, the extracellular N-terminus of Gpr124 comprises multiple protein-protein interaction domains whose contributions to receptor function remain largely elusive. Specifically, the Gpr124 ectodomain is sequentially composed of an N-terminal LRR/CT domain, an Ig-like domain and a hormone receptor motif (HRM) preceding the membrane-proximal GPS-containing GAIN domain. The Gpr124 LRR/CT domain contains four leucine-rich repeat (LRR) units which are 20-29 residue-long structural units that assemble in a superhelical manner with tandemly arranged repeats to form curved solenoid structures acting as protein interaction frameworks. As found in Gpr124, extracellular LRR motifs are often flanked by cysteine-rich C-terminal domains (LRR-CTs) that are integral parts of the LRR domain and shield the hydrophobic core of the last LRR motif. Building a proper understanding of Gpr124 function will benefit from delineating the contribution of each N-terminal domain to receptor function.

The *adgra2* variant found in *ouchless* mutants differs from *adgra2* reference sequences by four non-synonymous SNPs as well as a 72 bp deletion corresponding to exon 4 (Figure 3A). While the SNPs represent naturally occurring variations, the exon 4 skipping event is caused by an ENU-induced essential splice-site mutation at the exon 4–intron 4 boundary and was shown to result in  $Adgra2^{ouchless}$  inactivation (Bostaille et al., 2017). Exon 4 encodes the third LRR motif (LRR3) of the LRR/CT domain. In order to determine how the absence of LRR3 mechanistically impairs *Adgra2* function, we generated C-terminal EGFP-tagged versions of wild-type (WT) *Adgra2* as well as *ouchless* ( $Adgra2^{ouchless}$ ) and  $\Delta$ LRR3 ( $Adgra2^{\Delta LRR3}$ ) variants. This latter variant reproduces the exon 4 deletion found in *ouchless* in a WT allele of *adgra2*, and hence lacks the *ouchless*-associated SNPs (Bostaille et al., 2017). We first evaluated the functionality of the fusion proteins in brain angiogenic assays in zebrafish by mRNA injections at the one-cell stage. While ectopic restoration of either EGFP-tagged or untagged versions of WT *Adgra2* could restore angiogenic sprouting in *adgra2*<sup>s984/s984</sup> hindbrains (red arrowheads in Figure 3C), the equivalent  $Adgra2^{ouchless}$  and  $Adgra2^{\Delta LRR3}$  variants were inactive (Figure 3B,C). These observations extend and confirm previous findings indicating that C-terminal fusions are compatible with receptor function *in vivo* and that, in the absence of LRR3, *Adgra2* is non-functional (Vanhollebeke et al., 2015, Bostaille et al., 2017).

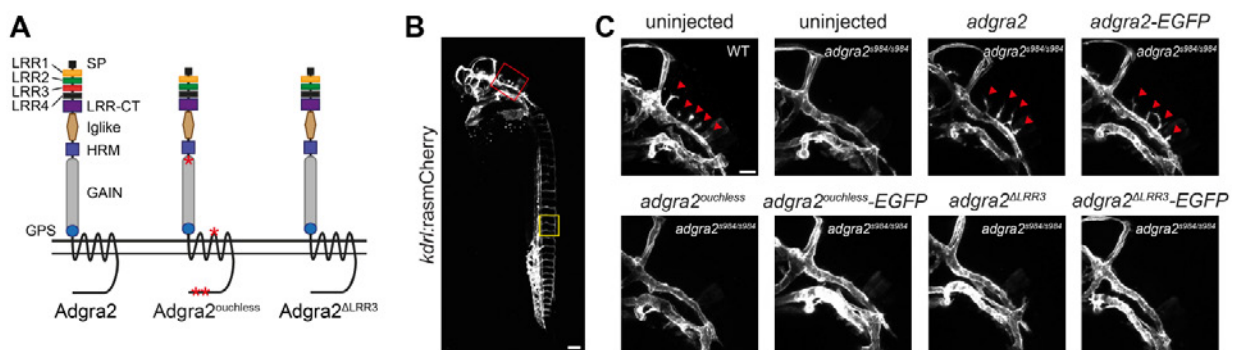


**Figure 3.**  $Adgra2^{ouchless}$  mislocalizes to the endoplasmic reticulum. (A) Schematic representation of *Adgra2*,  $Adgra2^{ouchless}$  and  $Adgra2^{\Delta LRR3}$  topology and domain organization.  $Adgra2^{ouchless}$  and  $Adgra2^{\Delta LRR3}$  lack the third LRR motif (red rectangle). The positions of the residue variations resulting from naturally occurring SNPs in  $adgra2^{ouchless}$  are designated by red asterisks. (B) Maximal intensity projection of a confocal z-stack of a WT *Tg(kdrl:ras-mCherry)* embryo at 36 hpf in lateral view. The red and yellow boxes define, respectively, the magnified areas of the hindbrain vasculature shown in C and the intersegmental vessels shown in E. Scale bar: 100  $\mu$ m. (C) Maximal intensity projection of a confocal z-stack of WT and *adgra2*<sup>s984/s984</sup> *Tg(kdrl:ras-mCherry)* embryos at 36 hpf in lateral view after injection of 100 pg of *adgra2*, *adgra2*-EGFP,  $adgra2^{ouchless}$ ,  $adgra2^{ouchless}$ -EGFP,  $adgra2^{\Delta LRR3}$  or  $adgra2^{\Delta LRR3}$ -EGFP mRNA at the one-cell stage. The red arrowheads point to the CtAs invading the hindbrain rhombomeres. Scale bar: 50  $\mu$ m.



We then analyzed the stability and subcellular distribution of the EGFP-tagged variants in different cell types. When examined in the large and cobblestone-shaped enveloping layer cells of the 5 h post fertilization (hpf) zebrafish blastula, WT Adgra2-EGFP labeled the plasma membrane where it colocalized with a membrane-tethered lyn-RFP marker. By contrast, the mutant fusion proteins accumulated in an intracellular reticulate compartment reminiscent of the ER. Similarly, when analyzed in ECs of mosaic transgenic zebrafish, the WT fusion decorated the EC plasma membranes, including the numerous filopodial extensions of the tip cells, while the mutant variants showed strong intracellular and perinuclear signals that did not colocalize with the ras-mCherry EC membrane marker. Finally, in order to streamline quantitative colocalization studies, we imaged the cellular distribution of the EGFP fusion proteins in cultured HEK293T cells. Whereas the WT fusion protein accumulated at the plasma membrane marked by GPI-RFP as anticipated, the mutant versions failed to reach this compartment but instead accumulated intracellularly. The accumulating compartment was identified as the ER with the help of the mCherry-fused ER protein translocation apparatus component SEC61 $\beta$ . This was further quantitatively evaluated by Pearson's colocalization coefficient (PCC) analysis. Moreover, a perfect correlation was observed between the capacity of the LRR chimera variants to reach the plasma membrane and their ability to support vascular sprouting in the zebrafish hindbrain or to induce the formation of DRG neurons.

When overexpressed in cultured cells, Adgra2 and Reck colocalize at the plasma membrane and proximity ligation assays further suggest that the proteins may directly interact within this compartment to assemble a receptor complex (Vanhollebeke et al., 2015). It remains to be determined whether the partners recognize and assist each other during their progression within the secretory pathway or instead meet at the plasma membrane after independent trafficking events. We took advantage of the ER retention of the LRR/CT variants to address this question. As revealed by indirect immunofluorescence assays in non-permeabilized HEK293T cells, HA-Reck reached the plasma membrane independently of the nature and trafficking status of the co-expressed Adgra2 receptor (**Figure 4A**). In addition, when expressed individually in HEK293T cells, Reck and Adgra2 localized to the plasma membrane (Vanhollebeke et al., 2015). These results suggest that Reck does not require Adgra2 in order to reach the plasma membrane and vice versa. However, as HEK293T cells express low levels of endogenous *ADGRA2* and *RECK* (Vanhollebeke et al., 2015; Zhou and Nathans, 2014), this endogenous protein pool might be sufficient to accompany ectopic Reck and/or Adgra2 during secretion. We therefore engineered *ADGRA2*<sup>-/-</sup> and *RECK*<sup>-/-</sup> HEK293T cells through CRISPR/Cas9 approaches and re-evaluated Adgra2 and Reck trafficking in these genetic backgrounds (**Figure 4B**). As in WT cells, both proteins accumulated at the plasma membrane when expressed individually, indicating that each partner can reach its final destination independently (**Figure 4C,D**).

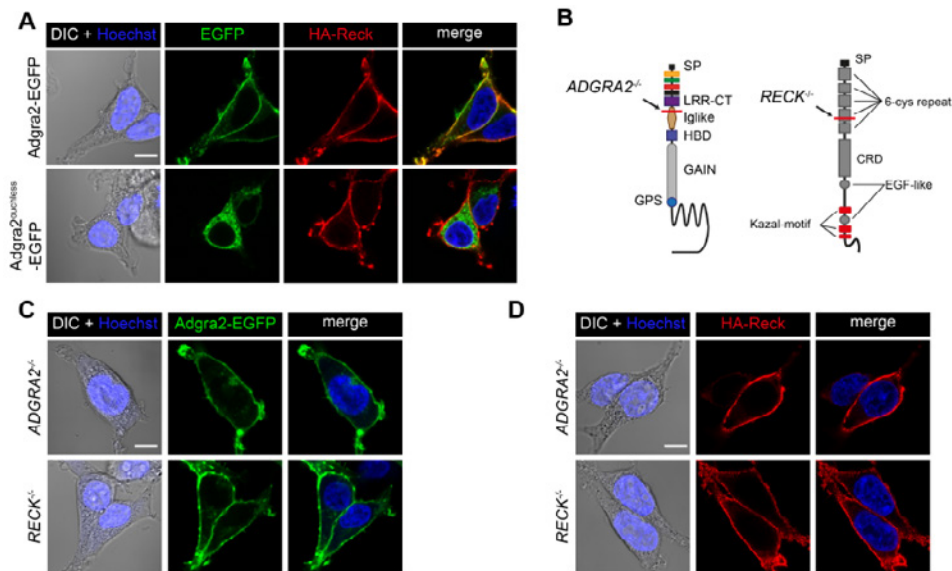


**Figure 4 Independent trafficking of Reck and Adgra2 to the plasma membrane.** (A) Single-plane confocal images of non-permeabilized HEK293T cells 48 h after transfection with *HA-reck* and *adgra2-EGFP* variants, as indicated. (B) Schematic representation of the genetic lesions of *ADGRA2*<sup>-/-</sup> and *RECK*<sup>-/-</sup> cells. The position of the frame-shift mutation is indicated by the red line. (C,D) Single-plane confocal images of non-permeabilized *ADGRA2*<sup>-/-</sup> and *RECK*<sup>-/-</sup> HEK293T cells 48 h after transfection with *adgra2-EGFP* (C) and *HA-reck* (D) constructs. In all panels, EGFP is detected by direct fluorescence and the HA-Reck fusion by anti-HA indirect immunofluorescence. Cells were additionally transfected with a *Wnt7a* (mouse gene) expression construct. Nuclei were counterstained with Hoechst. Scale bars: 10  $\mu$ m.

When assessed 48 h post transfection in saponin-permeabilized HEK293T cells, a minor fraction of HA-Reck can be immunodetected in the ER and as such co-distributes with *Adgra2*<sup>ouchless</sup> (Figure 5A, arrows) and presumably with a fraction of WT *Adgra2* transiting through this compartment. To test whether *Adgra2* is able to interact with *Reck* under these conditions, we performed proximity ligation assays as described previously (Vanhollebeke et al., 2015). As shown in Figure 5B, no interaction could be detected between HA-Reck and FLAG-*Adgra2*<sup>ouchless</sup>, in contrast to the plasma membrane-localized signal readily detected in HA-Reck and FLAG-*Adgra2* co-expressing cells. These results suggest that either the ER is not permissive for the formation of the complex or that the LRR deletion in *Adgra2* impairs its interaction with *Reck*.

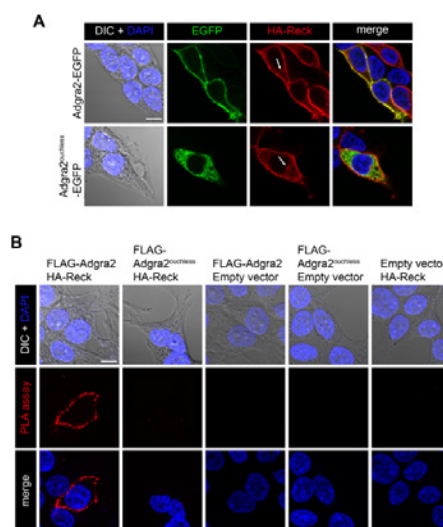


**Figure 5 Cellular distribution of *Adgra2* and *Reck* interaction.** (A) Single-plane confocal images of saponin-permeabilized HEK293T cells 48 h after transfection with *HA-reck* and *adgra2-EGFP* variants, as indicated. Nuclei were counterstained with DAPI. EGFP is detected by direct fluorescence and the HA-Reck fusion by anti-HA indirect immunofluorescence. Arrows point to the ER. (B) Proximity ligation assays in HEK293T cells 48 h after transfection with *FLAG-adgra2*, *FLAG-adgra2*<sup>ouchless</sup> and *HA-reck* constructs, as indicated. Nuclei were counterstained with DAPI. In all panels, cells were additionally transfected with a *Wnt7a* (mouse gene) expression construct. Scale bar: 10  $\mu$ m.

This study characterized the functionally null mutation of *adgra2* recently identified in zebrafish *ouchless* mutants. The genetic lesion results in *adgra2* alternative splicing and we show that this receptor variant localizes to the ER instead of the plasma membrane. This unprecedented occurrence of an aberrantly routed Adgra2 prompted us to evaluate whether the intracellular trafficking of Reck and Adgra2 are interdependent. When co-expressed with the ER-retained Adgra2 variant, Reck still reached the plasma membrane. Extending this analysis in CRISPR/Cas9 engineered cells, Reck was shown to accumulate at the plasma membrane in both WT and *ADGRA2*<sup>-/-</sup> HEK293T cells and, similarly, Adgra2 trafficking to the plasma membrane was unaffected by the presence or absence of RECK. These data indicate that the partners, when expressed individually, are able to traffic independently. When co-expressed in HEK293T cells, their close proximity can be detected by PLA assays at the plasma membrane but not within the endomembrane compartments of the secretory pathway through which they transit. These combined observations indicate that the partners first meet at the plasma membrane and that their synergy is likely restricted to the events occurring subsequently at the cell surface, in agreement with the current model (Vanhollebeke et al., 2015). It is conceivable that the interaction between Adgra2 and Reck is only made possible within plasma membrane microdomains of specific proteolipidic composition or that a yet to be defined component induces complex formation within this compartment. The selective association of Reck and Adgra2 at the plasma membrane could also result from the higher concentrations reached within this final membrane compartment favoring the potentially transient encounters of the partners.

While this study describes the role of the LRR/CT domain in promoting Adgra2 progression through the ER, it does not exclude additional roles for this domain in the Adgra2/Reck signaling pathway. The LRR/CT domain might, for instance, be additionally implicated in the interactions with Reck, Wnt7 or Fzd/Lrp5/6 occurring at the plasma membrane.

### **3.3. Defining the molecular mechanism for Wnt ligand-specific signaling controlling brain vascularization in vertebrates (Eubelen et al. Science)**

As outlined above, Wnt signaling is an ancient signaling pathway that has accompanied the emergence of metazoans and is key to many developmental, physiological, and disease processes. Similar to other signaling pathways, gene families for both Wnt ligand and its corresponding Frizzled receptor have undergone extensive expansion during metazoan evolution. Vertebrate genomes harbor 19 closely related Wnt genes as well as 10 Frizzled genes. Gene duplication is typically considered a major driving force in the evolution of new biological functions through neo- or subfunctionalization of emerging paralogs. How this functional diversification of Wnt ligands is structurally and molecularly organized, however, remains poorly understood. The Wnt/Frizzled molecular interaction is mediated by residues conserved across both families. This promiscuous interaction is incompatible with monospecific recognition and, accordingly, when tested in pair-wise combinations, multiple Wnt ligands compete for binding to various Frizzled receptors.

These observations raise the questions of how Wnt ligands achieve functional diversification and how cells interpret the intermingled expression patterns of simultaneous and sometimes conflicting Wnt signals. In some biological settings, cells may integrate all signaling inputs non discriminately and trigger appropriate responses by considering their total net balance. However, other biological processes exhibit strict Wnt ligand selectivity, despite complex Wnt/Frizzled expression landscapes. A prototypical example is provided by the exclusive control of mammalian forebrain and ventral spinal cord angiogenesis by Wnt7a and Wnt7b.

Within this neurovascular unit, in order to respond to neural progenitor-derived Wnt7 by activating Wnt/b-catenin signaling, cerebral endothelial cells must express a membrane protein complex consisting of the adhesion G protein-coupled receptor (GPCR) Gpr124 (Adgra2) and the glycosylphosphatidylinositol-anchored glycoprotein Reck. This Gpr124/Reck complex was recently reported to promote Wnt7-specific responses.

Using a combination of biophysical approaches and ligand-binding assays in genetically engineered cells, we demonstrated that ligand selectivity is conferred by Reck, which mediates Wnt7-specific binding in a Frizzled-independent manner. Reck orchestrates Wnt ligand discrimination by engaging the structurally disordered and highly divergent linker domain of Wnt7. The presence of Gpr124 is required to deliver Reck-bound Wnt7 to Frizzled by assembling higher-order Reck/Gpr124/Frizzled/Lrp5/6 complexes. This Gpr124 tethering function does not rely on its GPCR structure but instead on its combined capacity to interact with Reck extracellularly and recruit the Dishevelled scaffolding protein intracellularly. By bridging Gpr124 and Frizzled, Dishevelled recruits Wnt7, via its association with Reck, into dynamic Wnt/Frizzled signalosomes, resulting in increased local concentrations of ligand available for Frizzled signaling.

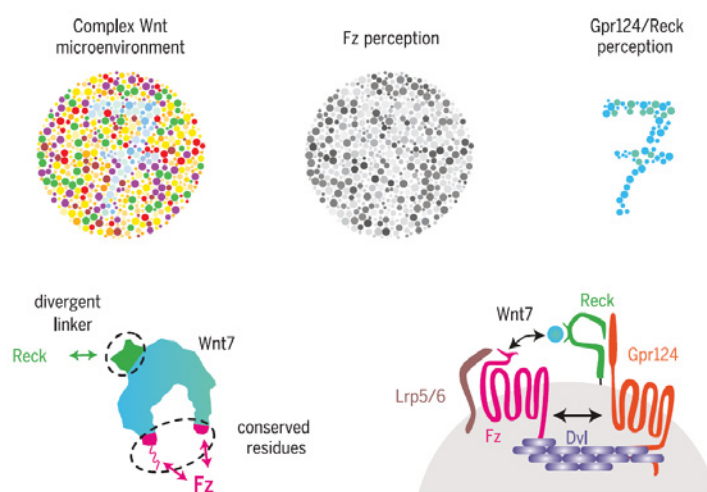


**Figure 6** Task sharing for orchestrated Wnt7-specific cellular responses. (Top) Gpr124 and Reck cooperatively alter the cell's perception of its Wnt microenvironment by selectively potentiating Wnt7 signals (cyan-tinted dots). (Bottom) Reck decodes Wnt ligands by establishing monospecific contacts with the highly divergent Wnt7 linker domain. Gpr124 links Reck-bound Wnt7 to Dishevelled. Dishevelled polymers by interacting simultaneously with Gpr124 and Fz assemble Wnt7-enriched signalosomes that trigger signaling through Fz receptors and Lrp5/6 co-receptors.

Our data reveal that cells are equipped with “Wnt-decoding modules” that distinguish between Wnt ligands that are otherwise very similar. They also reveal a critical role for the linker domain in Wnt ligand evolution and functional diversification. These mechanistic insights into the Wnt decoding capacities of vertebrate cells predict that additional Wnt decoding modules exist, enabling fine-tuning of cellular behaviors in response to other Wnt or Frizzled family members. These modules expand the diversity of proximal events in Wnt signaling, opening new therapeutic opportunities for conditions in which Wnt stimulation or inhibition are desirable at the membrane level. In particular, the mechanisms uncovered here provide an opportunity for the targeted treatment of human central nervous system neurovascular disorders.

### 3.4. Probing the function of endothelial Wnt/ $\beta$ -catenin in brain vessel anastomosis and maturation (Hübner et al. Nat. Commun. 2018)

The above mentioned Wnt/ $\beta$ -catenin signaling mechanism is essential for brain vascular invasion. Upon disruption, vertebrate brains exhibit profound CNS-specific vascular defects. This signaling pathway is considered as a master regulator of CNS vascular biology and further functions are suspected at later steps of the establishment of the cerebrovasculature. In search for these functions, we contributed to a study that investigated the subsequent requirements of Wnt/ $\beta$ -catenin signaling during CNS blood vessel morphogenesis and maturation. Canonical Wnt signaling is crucial for vascularization of the central nervous system and blood-brain barrier (BBB) formation. BBB formation and modulation are

not only important for development, but also relevant for vascular and neurodegenerative diseases. However, there is little understanding of how Wnt signaling contributes to brain angiogenesis and BBB formation. Here we show, using high resolution *in vivo* imaging and temporal and spatial manipulation of Wnt signaling, different requirements for Wnt signaling during brain angiogenesis and BBB formation. In the absence of Wnt signaling, premature Sphingosine-1-phosphate receptor (S1pr) signaling reduces VE-cadherin and Esama at cell-cell junctions (Figure 7). We suggest that Wnt signaling suppresses S1pr signaling during angiogenesis to enable the dynamic junction formation during anastomosis, whereas later S1pr signaling regulates BBB maturation and VE-cadherin stabilization. Our data provides a link between brain angiogenesis and BBB formation and identifies Wnt signaling as coordinator of the timing and as regulator of anastomosis.

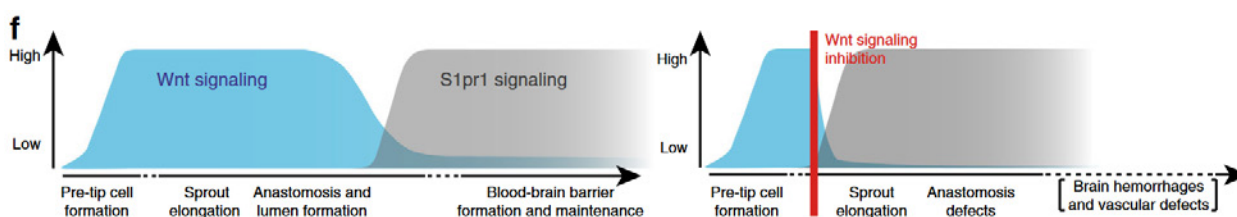
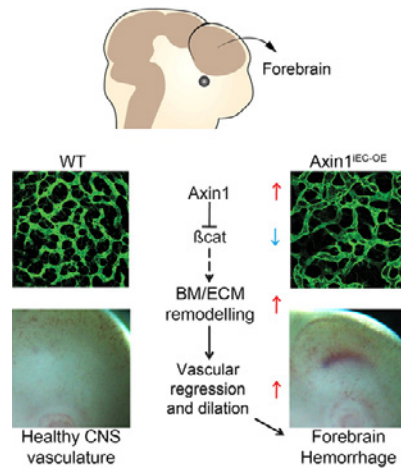


Figure 7. Illustration of Wnt and S1pr1 signaling during brain vascularization in wild type and Wnt-depleted embryos.

### 3.5. Probing the function of endothelial Wnt/ $\beta$ -catenin in BBB maintenance (Jensen et al. ATVB. 2019)

Besides the early functions described in 3.4, we contributed to a study that analyzed the later aspects of BBB maintenance under control of Wnt/ $\beta$ -catenin signaling. The Wnt/ $\beta$ -catenin pathway orchestrates development of the blood-brain barrier, but the downstream mechanisms involved at different developmental windows and in different central nervous system (CNS) tissues have indeed remained elusive. Here, we create a new mouse model allowing spatiotemporal investigations of Wnt/ $\beta$ -catenin signaling by induced overexpression of Axin1, an inhibitor of  $\beta$ -catenin signaling, specifically in endothelial cells (Axin1 iEC-OE). AOE (Axin1 overexpression) in Axin1 iEC- OE mice at stages following the initial vascular invasion of the CNS did not impair angiogenesis but led to premature vascular regression followed by progressive dilation and inhibition of vascular maturation resulting in forebrain-specific hemorrhage 4 days post-AOE. Analysis of the temporal Wnt/ $\beta$ -catenin driven CNS vascular development in zebrafish also suggested that Axin1 iEC- OE led to CNS vascular regression and impaired maturation but not inhibition of ongoing angiogenesis within the CNS. Transcriptomic profiling of isolated,  $\beta$ -catenin signaling-deficient endothelial cells during early blood-brain barrier-development (E11.5) revealed ECM (extracellular matrix) proteins as one of the most severely deregulated clusters. Among the 20 genes constituting the forebrain endothelial cell-specific response signature, 8 ( Adamtsl2, Apod, Ctsw, Htra3, Pglyrp1, Spock2, Ttyh2, and Wfdc1) encoded bona fide ECM proteins. This specific  $\beta$ -catenin-responsive ECM signature was also repressed in Axin1 iEC- OE and endothelial cell-specific  $\beta$ -catenin-knockout mice ( Ctnnb1-KO<sub>iEC</sub>) during initial blood-brain barrier maturation (E14.5), consistent with an important role of Wnt/ $\beta$ -catenin signaling in orchestrating the development of the forebrain vascular ECM. These results of this study suggest a novel mechanism of establishing a CNS endothelium-specific ECM signature downstream of Wnt- $\beta$ -catenin that impact spatiotemporally on blood-brain barrier differentiation during forebrain vessel development.



**Figure 8.** Wnt signaling inhibition in CNS endothelial cells triggers basement membrane/extracellular matrix remodelling that lead to vascular regression and dilation

### 3.6. Assessing the spatial heterogeneity of endothelial cell maturation signaling in the vertebrate brain (Benz et al, eLife 2019).

Not all blood vessels in the brain develop BBB properties, in particular those that mediate communication with the periphery in secretory or sensory circumventricular organs. In this collaborative study we started to characterize how blood vessels in these organs escape from the BBB-inductive signaling events. The circumventricular organs (CVOs) in the central nervous system (CNS) lack a vascular blood-brain barrier (BBB), creating communication sites for sensory or secretory neurons, involved in body homeostasis. Wnt/ $\beta$ -catenin signaling is essential for BBB development and maintenance in endothelial cells (ECs) in most CNS vessels. Here we show that in mouse development, as well as in adult mouse and zebrafish, CVO ECs rendered Wnt-reporter negative, suggesting low level pathway activity. Characterization of the subfornical organ (SFO) vasculature revealed heterogenous claudin-5 (Cldn5) and Plvap/Meca32 expression indicative for tight and leaky vessels, respectively. Dominant, EC-specific  $\beta$ -catenin transcription in mice, converted phenotypically leaky into BBB-like vessels, by augmenting Cldn5+ vessels, stabilizing junctions and by reducing Plvap/Meca32+ and fenestrated vessels, resulting in decreased tracer permeability. Endothelial tightening augmented neuronal activity in the SFO of water restricted mice. Hence, regulating the SFO vessel barrier may influence neuronal function in the context of water homeostasis.

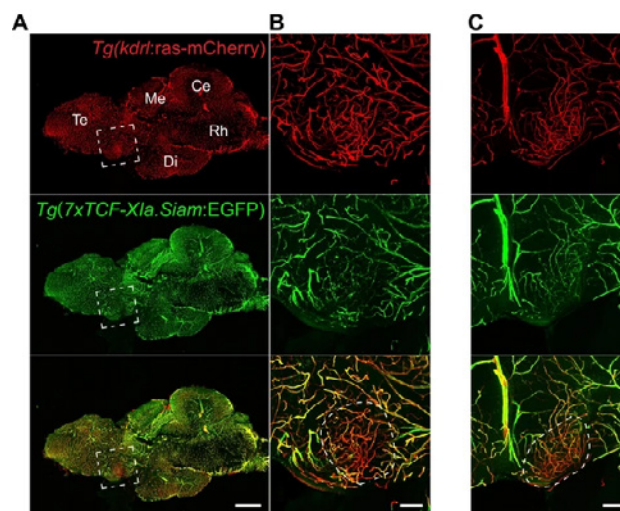


**Figure 9.** Low Wnt/ $\beta$ -catenin signaling in the adult circumventricular organs allows for efficient communication between the CNS and the peripheral organs, as illustrated here for the OVLT (organum vasculosum of the lamina terminalis) of adult zebrafish.

## 4. Outlook

---

Based on the previous findings, our project will continue to study brain angiogenesis and blood-brain barrier formation at the single-cell and real-time resolution in order to unravel the mechanisms through which neural signaling molecules couple brain vascular invasion and barrierogenesis.

## 5. Publications

---

- Jensen LD, Hot B, Ramsköld D, Germano RFV, Yokota C, Giatrellis S, Lauschke VM, Hubmacher D, Li MX, Hupe M, Arnold TD, Sandberg R, Frisé J, Trusohamn M, Martowicz A, Wisniewska-Kruk J, Nyqvist D, Adams RH, Apte SS, Vanhollebeke B, Stenman JM, Kele J. Disruption of the Extracellular Matrix Progressively Impairs Central Nervous System Vascular Maturation Downstream of  $\beta$ -Catenin Signaling. *Arterioscler Thromb Vasc Biol*. 2019 Jul;39(7):1432-1447.
- Morgan RK, Anderson GR, Araç D, Aust G, Balenga N, Boucard A, Bridges JP, Engel FB, Formstone CJ, Glitsch MD, Gray RS, Hall RA, Hsiao CC, Kim HY, Knierim AB, Kusluri DK, Leon K, Liebscher I, Piao X, Prömel S, Scholz N, Srivastava S, Thor D, Tolias KF, Ushkaryov YA, Vallon M, Van Meir EG, Vanhollebeke B, Wolfrum U, Wright KM, Monk KR, Mogha A. The expanding functional roles and signaling mechanisms of adhesion G protein-coupled receptors. *Ann N Y Acad Sci*. 2019 Nov;1456(1):5-25.
- Campenhout CV, Cabochette P, Veillard AC, Laczik M, Zelisko-Schmidt A, Sabatel C, Dhainaut M, Vanhollebeke B, Gueydan C, Krus V. Guidelines for optimized gene knockout using CRISPR/Cas9. *Biotechniques*. 2019 Jun;66(6):295-302.
- Benz F, Wichitnaowarat V, Lehmann M, Germano RF, Mihova D, Macas J, Adams RH, Taketo MM, Plate KH, Guérit S, Vanhollebeke B, Liebner S. Low wnt/ $\beta$ -catenin signaling determines leaky vessels in the subfornical organ and affects water homeostasis in mice. *Elife*. 2019 Apr 1;8. pii: e43818.
- Bonnin E<sup>§</sup>, Cabochette P<sup>§</sup>, Filosa A, Jühlen R, Komatsuzaki S, Hezwani M, Dickmanns A, Martinelli V, Vermeersch M, Supply L, Martins N, Pirenne L, Ravenscroft G, Lombard M, Port S, Spillner C, Janssens S, Roets E, Van Dorpe J, Lammens M, Kehlenbach RH, Ficner R, Laing NG, Hoffmann K, Vanhollebeke B<sup>#</sup>, Fahrenkrog B<sup>#</sup>. Biallelic mutations in nucleoporin NUP88 cause lethal fetal akinesia deformation sequence. *PLoS Genet*. 2018 Dec 13;14(12):e1007845. doi: 10.1371/journal.pgen.1007845. <sup>§</sup> co-first authors, <sup>#</sup> co-corresponding authors.
- Hübner K, Cabochette P, Diéguez-Hurtado R, Wiesner C, Wakayama Y, Grassme KS, Hubert M, Guenther S, Belting HG, Affolter M, Adams RH, Vanhollebeke B, Herzog W. Wnt/ $\beta$ -catenin signaling regulates VE-cadherin-mediated anastomosis of brain capillaries by counteracting S1pr1 signaling. *Nat Commun*. 2018 Nov 19;9(1):4860. doi: 10.1038/s41467-018-07302-x.
- Eubelen M<sup>§</sup>, Bostaille N<sup>§</sup>, Cabochette P, Gauquier A, Tebabi P, Dumitru AC, Koehler M, Gut P, Alsteens D, Stainier DYR, Garcia-Pino A, Vanhollebeke B. A molecular mechanism for Wnt ligand-specific signaling. *Science*. 2018 Aug 17;361(6403). pii: eaat1178. doi: 10.1126/science.aat1178. <sup>§</sup> co-first authors
- Guerra A, Germano RF, Stone O, Arnaout R, Guenther S, Ahuja S, Uribe V, Vanhollebeke B, Stainier DY, Reischauer S. Distinct myocardial lineages break atrial symmetry during cardiogenesis in zebrafish. *eLife*. 2018 May 15;7. pii: e32833. doi: 10.7554/eLife.32833.
- Bostaille N, Gauquier A, Stainier DY, Raible DW, Vanhollebeke B. Defective *adgra2* (*gpr124*) splicing and function in zebrafish *ouchless* mutants. *Development*. 2017 Jan 1;144(1):8-11.
- Bostaille N, Gauquier A, Twyffels L, Vanhollebeke B. Molecular insights into *Adgra2/Gpr124* and *Reck* intracellular trafficking. *Biol Open*. 2016 Dec 15;5(12):1874-1881.
- Fontaine F, Lecordier L, Vanwalleghe G, Uzureau P, Van Reet N, Fontaine M, Tebabi P, Vanhollebeke B, Büscher P, Pérez-Morga D, Pays E. APOLs with low pH dependence can kill all African trypanosomes. *Nat Microbiol*. 2017 Nov;2(11):1500-1506.
- Horáková E, Changmai P, Vancová M, Sobotka R, Van Den Abbeele J, Vanhollebeke B, Lukeš J. The *Trypanosoma brucei* TbHrg protein is a heme transporter involved in the regulation of stage-specific morphological transitions. *J Biol Chem*. 2017 Apr 28;292(17):6998-7010.
- De Muylder G, Vanhollebeke B, Caljon G, Wolfe AR, McKerrow J, Dujardin JC. Naloxonazine, an Amastigote-Specific Compound, Affects *Leishmania* Parasites through Modulation of Host-Encoded Functions. *PLoS Negl Trop Dis*. 2016 Dec 30;10(12):e0005234.

## 6. Additional References

---

- Anderson K. D., Pan L., Yang X., Hughes V. C., Walls J. R., Dominguez M. G., Simmons M. V., Burfeind P., Xue Y., Wei Y. et al. (2011). Angiogenic sprouting into neural tissue requires Gpr124, an orphan G protein-coupled receptor. **Proc. Natl. Acad. Sci. USA** 108, 2807-2812. 10.1073/pnas.1019761108
- Bostaille N., Gauquier A., Stainier D. Y. R., Raible D. W. and Vanhollebeke B. (2017). Defective *adgra2* (*gpr124*) splicing and function in zebrafish *ouchless* mutants. **Development**, doi:10.1242/dev.146803. 10.1242/dev.146803
- Bostaille N, Gauquier A, Twyffels L, Vanhollebeke B. Molecular insights into Adgra2/Gpr124 and Reck intracellular trafficking. **Biol Open**. 2016 Dec15;5(12):1874-1881.
- Cullen M., Elzarrad M. K., Seaman S., Zudaire E., Stevens J., Yang M. Y., Li X., Chaudhary A., Xu L., Hilton M. B. et al. (2011). GPR124, an orphan G protein-coupled receptor, is required for CNS-specific vascularization and establishment of the blood-brain barrier. **Proc. Natl. Acad. Sci. USA** 108, 5759-5764. 10.1073/pnas.1017192108
- de Almeida G. M., Yamamoto M., Morioka Y., Ogawa S., Matsuzaki T. and Noda M. (2015). Critical roles for murine Reck in the regulation of vascular patterning and stabilization. **Sci. Rep.** 5, 17860 10.1038/srep17860
- Kuhnert F., Mancuso M. R., Shamloo A., Wang H.-T., Choksi V., Florek M., Su H., Fruttiger M., Young W. L., Heilshorn S. C. et al. (2010). Essential regulation of CNS angiogenesis by the orphan G protein-coupled receptor GPR124. **Science** 330, 985-989. 10.1126/science.1196554
- Malmquist, S. J., Abramsson, A., McGraw, H. F., Linbo, T. H. and Raible, D. W. (2013). Modulation of dorsal root ganglion development by ErbB signaling and the scaffold protein Sorbs3. **Development** 140, 3986-3996. doi:10.1242/dev.084640
- Posokhova E., Shukla A., Seaman S., Volate S., Hilton M. B., Wu B., Morris H., Swing D. A., Zhou M., Zudaire E. et al. (2015). GPR124 functions as a WNT7-specific coactivator of canonical  $\beta$ -catenin signaling. **Cell Rep.** 10, 123-130. 10.1016/j.celrep.2014.12.020
- Ulrich F., Carretero-Ortega J., Menendez J., Narvaez C., Sun B., Lancaster E., Pershad V., Trzaska S., Veliz E., Kamei M. et al. (2016). Reck enables cerebrovascular development by promoting canonical Wnt signaling. **Development** 143, 147-159. 10.1242/dev.123059
- Vanhollebeke B., Stone O. A., Bostaille N., Cho C., Zhou Y., Maquet E., Gauquier A., Cabochette P., Fukuhara S., Mochizuki N. et al. (2015). Tip cell-specific requirement for an atypical Gpr124- and Reck-dependent Wnt/ $\beta$ -catenin pathway during brain angiogenesis. **eLife** 4, e06489 10.7554/eLife.06489
- Zhou Y. and Nathans J. (2014). Gpr124 controls CNS angiogenesis and blood-brain barrier integrity by promoting ligand-specific canonical Wnt signaling. **Dev. Cell** 31, 248-256. 10.1016/j.devcel.2014.08.018